Original Research

Study on Adsorption Characteristics of Heavy Metal Cd²⁺ by Biochar Obtained from *Water Hyacinth*

Xiaoshu Wang[1], Xiaomeng Guo[2,3], Tongtong Li[2], Jia Zhu[1], Jun Pang[2], Jianfeng Xu[2], Jinsheng Wang[4], Xuquan Huang[5], Jingsi Gao[1]*, Lei Wang [1,2]**

[1]School of Materials & Environmental Engineering, Institute of Urban Ecology and Environment Technology, Shenzhen Polytechnic, Shenzhen 518055, P.R. China
[2]State Key Laboratory of Environmental Criteria and Risk Assessment, Chinese Research Academy of Environmental Sciences, Beijing 100012, P.R. China
[3]The Guangxi Key Laboratory of Theory and Technology for Environmental Pollution Control, Guilin University of Technology, Guilin 541004, P.R. China
[4]Shenzhen BeiYu Environmental Technology Co., Ltd, Shenzhen 518063, P.R. China
[5]College of Hydraulic and Environmental Engineering, China Three Gorges University, Yichang 443002, P.R. China

Abstract

In this paper, the biochar prepared by pyrolysis biomass of *Water Hyacinth* were used as adsorption materials. The effects of initial concentration, adsorption temperature and electrolyte concentration on the adsorption process were analyzed. The adsorption effect of biochar prepared from the stem and root parts of biomass on Cd²⁺ in solution was investigated, and the interaction between leaching rule of alkali (earth) metal K⁺, Mg²⁺, Ca²⁺ and adsorption of heavy metal ions in the process of adsorption was studied. The results showed that the biochar prepared by pyrolysis of stem biomass (SBC) has a richer pore structure. Compared with the biochar prepared by root biomass (RBC), the specific surface area and pore volume of SBC increased by 25.85% and 27.91% respectively. This phenomenon indicated that SBC had a stronger adsorption effect than RBC. At 25ºC, the maximum adsorption capacity of RBC and SBC for Cd²⁺ was 77.20 mg g⁻¹ and 87.20 mg g⁻¹, respectively. Isothermal adsorption experiments and ionic strength experiments showed that the increase of temperature could promote the adsorption of Cd²⁺ by biochar. The adsorption process has a high degree of fitting with the Langmiur model, as well as the pseudo-second-order model. The adsorption sites were normally on the inner and outer surfaces of biochar, and the adsorption process was multi-molecular layer adsorption. In addition, the adsorption of Cd²⁺ by biochar had a correlation with the leaching of alkali (earth) metal in the system. In the adsorption process, the leaching of alkali (earth) metals was affected by the initial concentration of Cd²⁺ in the solution, and SBC leached more alkali (earth) metals than RBC, which proved that SBC has more

---

*e-mail: gaojingsi@szpt.edu.cn
**e-mail: wangleicraes@163.com

active sites and can replace heavy metals in the solution. This study proved that *Water Hyacinth* biochar owned characteristics of high recovery and low economic cost, which showed good adsorption to Cd^{2+} polluted wastewater and was feasible as a heavy metal adsorption material.

Introduction

In recent years, with the rapid development of urbanization and industrialization, more and more heavy metals entered into the water body directly or indirectly, causing serious pollution to the ecological environment [1, 2]. Most heavy metals are highly toxic, carcinogenic, bioaccumulative and non-biodegradable, especially the acute, subacute and chronic toxic effects of non-essential elements such as Hg, Cd, Pb, Cr, and As on organisms [3]. Once they accumulate in the human body through the biological chain, they pose a serious threat to human health [4, 5]. This irreversible damage is due to the internal stimulation of heavy metal to produce reactive oxygen species, and then produce a series of toxic effects on the organism, such as lipid peroxidation, mercapto protein consumption, and mutation and variation of genes [6]. Heavy metal cadmium (Cd) is a common pollutant in the environment, which mainly comes from various industrial activities such as electroplating, mining, smelting, printing and dyeing, and has high fluidity and durability [7, 8]. It is one of the most toxic metals in the environment, and cannot be eliminated only by relying on the self-purification ability of the natural environment [9], which is a major problem that needs to be solved urgently in the field of environment today. The main mechanism of Cd accumulation in organisms is through binding with Cd-binding proteins such as metallothionein [10]. What's more, it can interfere with the synthesis and secretion of hormones, which forms endocrine disrupting toxicity, increases oxidative stress and induces mitochondrial dysfunction [11]. At present, there are many conventional technologies for the disposal of cadmium-contaminated wastewater, including chemical precipitation, membrane removal, ion exchange, chelation and adsorption, etc [12-14].

Among these methods, adsorption is considered to be one of the most ideal methods due to its environmentally friendly characteristics [15-17]. Biochar is a carbon-rich solid produced by biomass pyrolysis in anoxic environment. In recent years, biochar has received extensive attention as a carbon-based adsorption material [18, 19]. The physical and chemical properties of biochar are mainly affected by the preparation conditions. The adsorption properties of biochar for heavy metals are mainly affected by specific surface area, pore structure and surface functional groups, etc. In addition, it is also related to coexisting ions in solution, pH value and initial concentration of heavy metal ions in solution [20]. Raw materials will form microporous structures due to the loss of moisture and volatile substances during pyrolysis [21]. Generally, the higher temperature can reach, the richer and denser the pore structure can be formed. However, some studies have found that a lower specific surface area may be generated at higher temperatures, which is due to tar generated from pyrolysis blocking the pore structures, resulting in a decrease in specific surface area [22]. There are many adsorption mechanisms for heavy metals by biochar. Currently, there are five mechanisms proposed and widely accepted, which include surface electrostatic adsorption, physical adsorption, surface complexation, surface precipitation, and ion exchange [23].

The relative contribution of the adsorption mechanism of biochar in the adsorption process depends largely on the preparation materials and adsorption conditions of biochar. There are many raw materials for the preparation of biochar, including livestock manure, straw, sawdust, distiller's grains, kitchen waste, and sludge, etc. The adsorption properties of materials prepared from different raw materials are quite different. Therefore, it is urgent to choose low-cost and environment-friendly raw materials to prepare adsorbent. *Water Hyacinth*, as an exotic species lacking natural enemies, has extremely strong growth and reproduction ability, which is widely distributed in rivers and lakes in South China, East China and Central China. A large amount of *Water Hyacinth* biomass is produced every year. If disposed of improperly, it will pose a threat to the environment as a waste. However, *Water Hyacinth*, as a raw material for preparing biochar, has natural advantages. its petioles part swelled like a gourd, and has a sponge-like structure with large cell gaps, which can generate a large specific surface area after pyrolysis. In addition, *Water Hyacinth* is rich in trace elements such as nitrogen, phosphorus, potassium, sodium, calcium and magnesium, which will produce abundant functional groups and more adsorption sites, and can effectively adsorb and retain heavy metals, reducing the harm of heavy metals to the environment [24-26].

Biochar prepared from hyacinth biomass was studied in this paper. Analyze the differences in physical and chemical properties of biochar prepared by pyrolysis of different parts of biomass. The effects of initial concentration, adsorption temperature and electrolyte concentration in solution on the adsorption of Cd^{2+} on biochar were confirmed by sequencing experiments. By analyzing the leaching concentration of alkali (earth) metal in biochar during adsorption, the interaction between alkali (earth) metal leaching and Cd^{2+} adsorption was clarified.
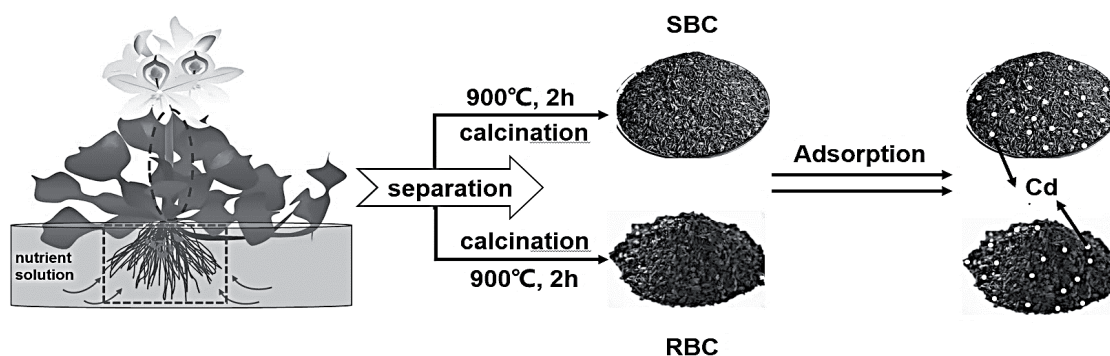
Fig. 1. The schematic diagram of synthesizing biochar and applying in heavy metal adsorption.

Experimental

Material Preparation

All the processes involved, including pre-treating biomass, calcining to produce biochar and adsorbing heavy metal, have been schematically illustrated in Fig. 1, which can ensure the highest conformity level. In this experiment, *Water Hyacinth* biomass was selected as raw material to prepare biochar. After a certain growing period, the biomass was harvested and separated from the root and steam parts. Then, the different organ biomasses were washed and dried to constant weight in the oven at 105ºC. The following operation is to obtain uniform biomass pellets by crushing with a grinder and passing through a 100 mesh sieve. Biomass was weighed and put in a crucible, then fed into tubular muffle furnace (KJ-T1200-S10400-LK). Under N_2 flow, the temperature rises to 900 ˚C at the rate of 10ºC min^{-1}. The calcination temperature is maintained for 2 hours, then cooled to room temperature and taken out, placed in a desiccator for reserve. The biochar prepared by pyrolysis of roots and stems was named RBC and SBC, respectively. And the biochar samples used in the experiment were all passed through a 100 mesh sieve, and the fine fraction was ready for the following characterization and series sorption experiments.

Characterization of Biochar

The specific surface area and pore volume of biochar were determined by automatic rapid surface area and pore size analyzer (ASAP2460). SEM-EDS scanning electron microscope (BCPCAS4800) was used to observe the surface and internal morphological characteristics of *Water Hyacinth* biochar as well as the types and contents of micro zone elements under different magnification. The crystal structure of the sample was analyzed by X-ray diffractometer (Bruker D8 Advance), the working conditions of the instrument were: Cu/Kα ray, tube voltage was 10 kV, tube current was 10 mA, working distance was 9 mm, scanning step was 0.026°, the scanning range is from 5° to 90°.

Sequencing Experiment

Effect of Initial Concentration on Adsorption of Cd²⁺ by Biochar

$Cd(NO_3)_2 \cdot H_2O$ was used to prepare Cd^{2+} solutions with initial concentration of 0, 5.00, 10.00, 15.00, 20.00, 25.00, 30.00, 50.00, 100.00, 200.00 and 500.00 mg L^{-1} respectively. $NaNO_3$ solution with 0.01 mol L^{-1} was used as supporting electrolyte, and the pH was adjusted to 5.5 [27-29] with HCl and NaOH. 0.02 g of SBC and RBC biochar were weighed and added into a 100.00 mL conical flask and add, and 20.00 mL of different concentrations of Cd^{2+} solution was added. They were placed in a constant temperature water bath oscillator and oscillated at 25ºC for 8 hours at 200 r min^{-1}. The supernatant was centrifuged and filtered by a filter equipped with a 0.45μm water system filter. The equilibrium concentration of Cd^{2+}, K^+, Ca^{2+}, Mg^{2+} in the clarified solution was determined by ICP-OES (iCAP 6000, Thermo). The adsorption equilibrium and removal rate of Cd^{2+} by biochar were calculated by formula (1) and formula (2), respectively, and the leaching amount of alkali (earth) metal was calculated by formula (3).

$$Q_e = \frac{C_0 - C_e}{m} \cdot V \qquad (1)$$

$$R = \frac{C_0 - C_e}{C_0} \times 100\% \qquad (2)$$

$$Q_t = \frac{C_2 - C_1}{m} \cdot V \qquad (3)$$

where: Q_e is the adsorption equilibrium amount of Cd^{2+}, mg g^{-1}; C_0 and C_e are the concentration of Cd^{2+} initial and adsorption equilibrium, respectively, mg L^{-1}; V is the solution volume, L; m is the mass of biochar, g; R is the removal rate of Cd^{2+}, %; Q_t is the amount of alkali (earth) metal leaching, mg g^{-1}; C_1 and C_2 are

the concentrations at the initial and adsorption equilibrium of the alkali (earth) metal, respectively, mg L^{-1}.

Isotherm and Kinetics Adsorption Experiment

Cd(NO$_3$)$_2$·H$_2$O was used to prepare Cd^{2+} solutions with initial concentration of 0, 5.00, 10.00, 15.00, 20.00, 25.00, 30.00 mg L^{-1} respectively. NaNO$_3$ solution with 0.01 mol L^{-1} was used as supporting electrolyte, and the pH was adjusted to 5.5 with HCl and NaOH. 0.02 g of SBC and RBC biochar were respectively weighed into a 100.00 mL conical flask and 20.00 mL of different concentrations of Cd^{2+} solution was added in the reactor. The isotherm adsorption experiments were conducted as follows: The mixture was placed in a constant temperature water bath oscillator and oscillated at 25ºC, 35ºC and 45ºC for 8 hours at 200 r min^{-1}. Kinetic experiments were implemented for contact time studies (0-1440 min) under the temperature of 25ºC. At fixed intervals, the supernatant was centrifuged and filtered by a filter equipped with a 0.45µm water system filter. The equilibrium concentration of Cd^{2+}, K$^+$, Ca^{2+}, Mg^{2+} in the clarified solution was determined by ICP-OES (iCAP 6000, Thermo). The equilibrium adsorption amount of biochar to Cd^{2+} was calculated by the formula (1).

The isotherm can describe the interaction between the adsorbent and the adsorbate, which is of great significance to the optimization of adsorbent materials and their application in practice.

Langmuir isotherm adsorption model is expressed as:

$$Q_e = \frac{Q_m b C_e}{1 + b C_e} \tag{4}$$

Freundlich isotherm adsorption model is expressed as:

$$Q_e = K_F C_e^{1/n} \tag{5}$$

where: Q_m refers to saturated adsorption capacity, mg·g^{-1}; which is an important index of the adsorption performance of the adsorbent; b is Langmuir adsorption characteristic constant L g^{-1}, which is a parameter to characterize the affinity between adsorbent and adsorbate, the larger the b value, the greater the adsorption affinity; K_F is the adsorption capacity parameter of Freundlich, and the value of n in the equation can be used as an indicator of the adsorption strength of biochar on heavy metal ions. The larger the K_F value, the greater the adsorption capacity, and the smaller the n value, the greater the adsorption capacity.

The kinetics of adsorption is used to predict the adsorption rate, which gives important information for designing and modeling the processes [30]. In this paper, two commonly used models were applied to determine the diffusion mechanism for Cd adsorption from aqueous solutions: the pseudo-first-order and pseudo-second-order models. The adsorption kinetics of Cd(II) onto biochar described by pseudo-first-order model and pseudo-second-order model are given in formulas (6) and (7).

$$\log\left(Q_e - Q_t\right) = \log Q_e - k_1 t \tag{6}$$

$$\frac{t}{Q_t} = \frac{1}{k_2 Q_e^2} + \frac{t}{Q_e} = \frac{1}{v_0} + \frac{t}{Q_e} \tag{7}$$

where: Q_e and Q_t (mg g^{-1}) are the adsorption capacity at equilibrium and at any time t (min). The constant k_1 (min^{-1}), k_2 (g mg^{-1} min^{-1}) are the adsorption rate constants of pseudo-first-order reaction, pseudo-second-order reaction, respectively. v_0 (mg g^{-1} min^{-1}) represents the initial reaction rate of adsorbing material.

Adsorption Experiments with Different Ionic Strengths

Different concentrations of NaNO$_3$ solution were used as supporting electrolytes for the adsorption process. Cd^{2+} solution with a concentration of 20.00 mg·L^{-1} was prepared with Cd(NO$_3$)$_2$·H$_2$O, and the pH was adjusted to 5.5 with HCl and NaOH. 0.02 g of SBC and RBC biochar were weighed and added into a 100.00 mL triangular conical flask, then 20.00 mL of Cd^{2+} solution was added with different electrolyte concentrations. They were placed in a constant temperature water bath oscillator and oscillated at 25ºC for 8 hours at 200 r min^{-1}. The supernatant was centrifuged and filtered by a filter equipped with a 0.45 µm water system filter. The equilibrium concentration of Cd^{2+}, K$^+$, Ca^{2+}, Mg^{2+} in the clarified solution was determined by ICP-OES (iCAP 6000, Thermo). The adsorption equilibrium and removal rate of Cd^{2+} by biochar were calculated by formula (1) and formula (2), respectively, and the leaching amount of alkali (earth) metal was calculated by formula (3).

Regeneration Experiments

Regeneration experiments was carried out in an alkaline environment. According to the adsorption condition parameters, adsorption experiment with 20 mg/L Cd(II) (20 mL) and 0.02 g SBC/RBC at pH 5.5 reached an equilibrium and washed with deionized water several times. Then, solutions containing 0.1 M NaOH was used to desorb Cd from the biochar during agitated on a shaker at 300 rpm and room temperature for 18 h. Samples were removed within a certain period of time for Cd detection determined by ICP-OES.

Table 1. Basic properties of *Water Hyacinth* biochar.

Sample	Yield (%)	Specific surface area (m^2 g^{-1})	Pore volume (cm^3 g^{-1})	Element concentrations (%)					
				C	O	Mg	Al	Si	Ca
RBC	45.21	217.05	0.145	61.71	21.86	1.02	2.36	5.44	5.88
SBC	33.48	273.16	0.196	71.89	14.46	1.71	0.34	3.59	6.77

Results and Discussion

Analysis and Characterization of Physical and Chemical Properties of Biochar

Analysis of Physical and Chemical Properties of Two Kinds of Biochar

Table 1 showed the yield and basic physical and chemical properties of RBC and SBC from pyrolysis of different parts of *Water Hyacinth*. The basic physical and chemical properties of biochar prepared from different parts of the raw materials were significantly different. In this paper, the yield was calculated as the ratio of biochar mass and the raw material mass. The yields of RBC and SBC were 45.21% and 33.48%, respectively.

Plant biomass was mainly composed of cellulose, hemicellulose and lignin, therefore, the difference in yield might be due to the different components of the pyrolysis feedstock. Studies have shown that the roots of *Water Hyacinth* biomass contain more abundant lignin, while the stem contains more cellulose and hemicellulose [31]. Cellulose and hemicellulose are more susceptible to pyrolysis than lignin, so the root yield is higher than that of stem. The presence of cellulose and hemicellulose is more conducive to the formation of pore structure of pyrolysis products [32], therefore SBC has larger specific surface area and pore volume than RBC, the former has a specific surface area of 273.16 m^2 g^{-1}, and the pore volume is 0.19 cm^3 g^{-1}, the latter has a specific surface area of 217.05 m^2 g^{-1} and a pore volume of 0.15 cm^3 g^{-1}, which increased by 25.85% and 27.91%, respectively. The adsorption of biochar mainly occurred on the inner and outer surfaces, and the specific surface area and pore structure are one of the important factors affecting the adsorption capacity [33]. In general, the larger the specific surface area of biochar, the larger the pore volume, which can provide more powerful conditions for adsorbing heavy metals, and the stronger the adsorption capacity.

SEM Combined with EDS Analysis of Biochar

Scanning electron microscopy (SEM) was used to observe the surface and internal morphology of biochar. The electron microscopic scans of RBC and SBC were
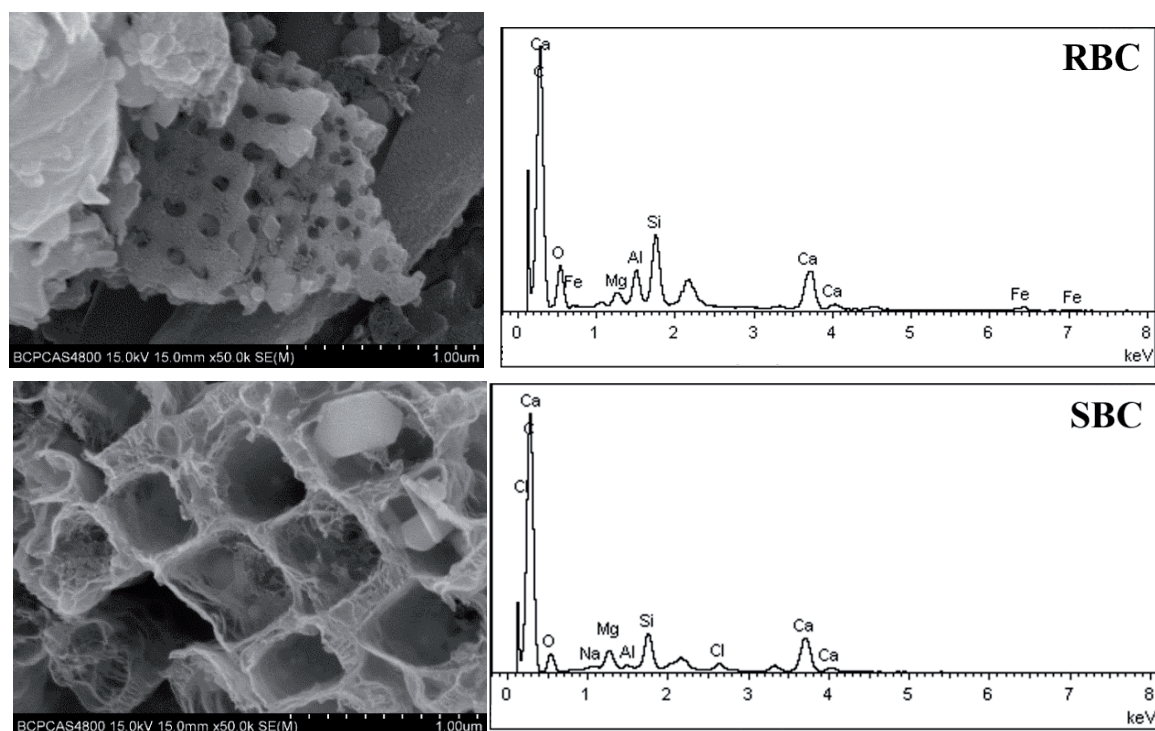

Fig. 2. SEM and EDS graphs of RBC and SBC.

shown in Fig. 2. *Water Hyacinth* petiole is expanded with spongy tissue with large cell gaps. After pyrolysis, SBC forms a porous regular bundle structure, in which pores are densely arranged and orderly, showing quadrangular shape, and the side length is about 4.50 μm. The root has a high lignin content and a dense structure. After pyrolysis, a variety of amorphous structures are formed in the RBC, and porous sheets are produced. The pore size of the pores in the sheet is about 1.10 μm, which may be caused by the pyrolysis of the cross-section of plant root duct structure. Comparing the two biochar materials from the microscopic morphology, combined with the specific surface area and pore volume measurement parameters of the two materials, it can be considered that SBC has a richer and more favorable pore structure than the RBC. It can be seen that the raw material is an important factor affecting the adsorption performance of biochar.

The EDS elemental analysis of the two kinds of biochar in Table 1 and Fig. 2 indicated that the carbon content of RBC was lower than that of SBC, while the oxygen content was higher than that of SBC, that is, the C/O ratio of SBC was greater than that of RBC, which indicated that SBC was deoxidized more completely after pyrolysis, while RBC contained more oxygen-containing functional groups. In addition, the two kinds of biochar contain Si, Ca, Mg, Al and other elements. The content of Si and Al in RBC were higher than that in SBC, while the content of Mg and Ca in SBC were higher than that in RBC. This difference is related to the raw material composition of biochar preparation.

XRD Analysis of the Two Kinds of Biochar

Fig. 3 showed the X-ray diffraction (XRD) patterns of RBC and SBC. By comparing the standard X-ray diffraction cards, it can be seen that the crystal structure of the two kinds of biochar is obviously different. The main crystals of RBC were SO_2 and $Ca_{0.5}Ai_2SiO_6 \cdot H_2O$ (orbital calcium zeolite). There were two weak peaks near $2\theta = 32°$ and $2\theta = 35°$, which belong to the diffraction peak of $AlCa_2Mg_{0.5}O_7Si_{1.5}$ (calcium magnesium aluminosilicate) [34]. The main crystalline phases in SBC were MgO and NaCl, and there were three obvious peaks near $2\theta = 27°$, $2\theta = 34°$ and $2\theta = 51°$. It belongs to the diffraction peak of Na_2SO_4, and $CaSO_4$ [35].

Effect of Initial Concentration on Adsorption of Cd^{2+} by Biochar

Effect of initial concentration on adsorption of Cd^{2+} by biochar RBC and SBC were shown in Fig. 4. It can be observed that the adsorption capacity of biochar RBC and SBC to Cd^{2+} increases gradually with the increase of initial concentration when the initial concentration of Cd^{2+} in solution is in a lower range $(0-200.00$ mg $L^{-1})$; The higher the initial concentration, the stronger the adsorption capacity of Cd^{2+}. The results show that biochar has multiple active sites on the surface when exposed to Cd^{2+} solution, which can be attributed to the unsaturated adsorption of biochar at low Cd^{2+} concentration. At this stage, the active sites on the surface of biochar are much higher than the content of Cd^{2+}. Because of the high
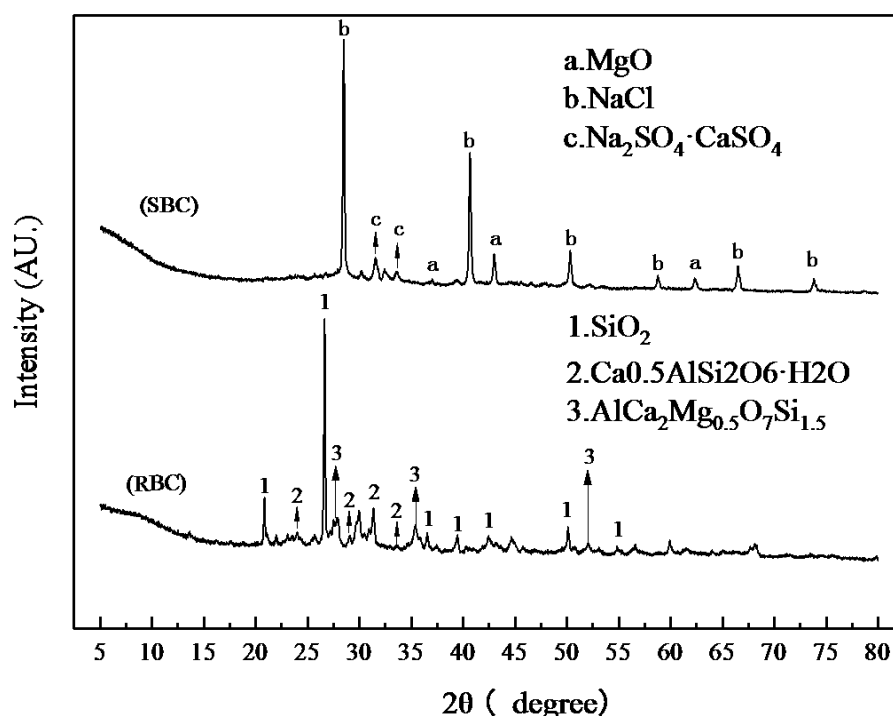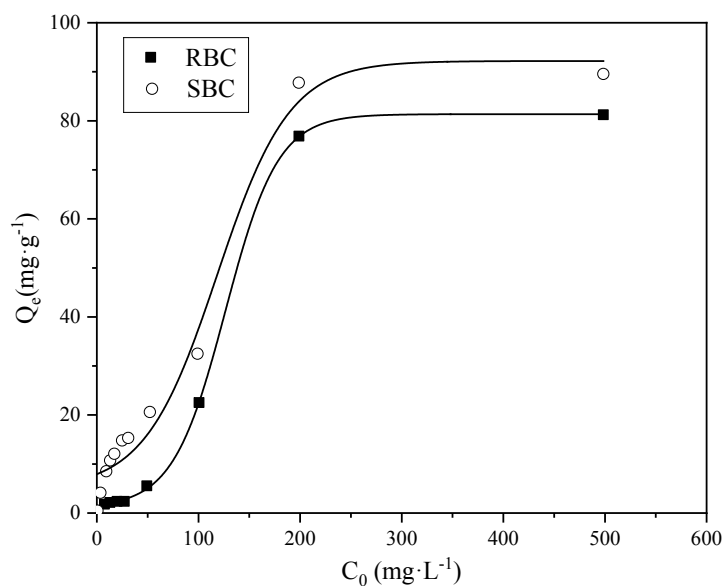

Fig. 3. XRD spectra of RBC and SBC.

Fig. 4. Effect of initial concentration on adsorption capacity of RBC and SBC.

affinity of the interaction, Cd^{2+} is captured very quickly, and the removal efficiency is high at this stage.

When the initial concentration reaches 200.00 mg L^{-1}, the adsorption capacity of the two kinds of biochar for Cd^{2+} changed little with the increase of concentration. The initial concentration of Cd^{2+} continues to rise, its speed gradually slows down and finally presents a stable trend with slight changes. The concentration of Cd^{2+} in the solution reaches a certain degree, the reaction equilibrium. The adsorption of biochar tends to be saturated, and the adsorption capacity of biochar to heavy metals reaches the maximum value, which means it no longer increases with the increase of initial concentration. The experimental data showed that the maximum adsorption capacity of RBC and SBC can reach 77.20 mg g^{-1} and 87.20 mg g^{-1} respectively. At different initial concentrations, the removal ability of biochar to Cd^{2+} was obviously different, which may be caused by mass transfer effects. The higher the concentration of Cd^{2+} ions in solution, the stronger the driving force of mass transfer, which increases the driving force of adsorption on the surface of biochar,

enhances the influence of diffusion flow, and promotes the removal of Cd^{2+} by adsorbents [36]. The maximum adsorption capacity of RBC and SBC detected from the actual experiments are relatively higher than the one observed for activated carbon, zeolite, sawdust, chitosan, and dairy manure biochar (Table 2).

It can also be seen from Fig. 4 that at the same initial concentration, the adsorption performance of the two kinds of biochar always presents SBC>RBC. Especially when the initial concentration of Cd^{2+} was 25.00 mg L^{-1}, the adsorption capacities of RBC and SBC were 1.86 mg g^{-1} and 15.15 mg g^{-1}, respectively. SBC was 8.14 times of RBC, which was consistent with BET, pore volume and SEM test results, indicating that compared with RBC, SBC has more developed pore structure and stronger adsorption performance.

Effect of Electrolyte Strength on Biochar Adsorption in Solution

Considering that there are many cations in industrial wastewater and polluted groundwater, the existence

Table 2. Comparison of Cd adsorption effect onto RBC and SBC with other adsorbents.

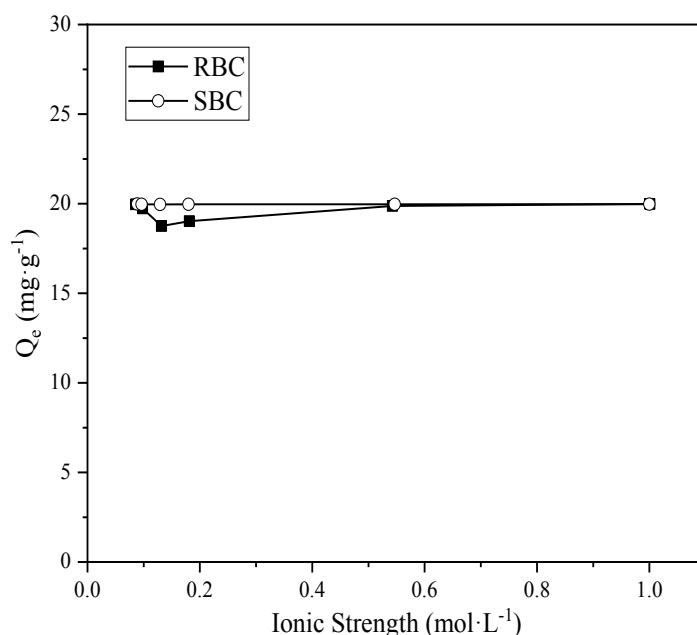| Material	Sources	Heavy metal	The adsorption amount
Activated carbon	Sabela et al., 2016 [37]	Cu(II)	75.0 mg g^{-1}
Zeolite from coal fly ash	Ifeoma et al, 2020 [38]	Cd(II)	39.01 mg g^{-1}
Sawdust	Gupta and Babu, 2009 [39]	Cr(VI)	41.5 mg g^{-1}
Chitosan from chemical agent	Asandei et al., 2009 [40]	Pb(II)	47.39 mg g^{-1}
Biochar from dairy manure	Xu et al., 2013 [41]	Cd(II)	51.4 mg g^{-1}
Biochar from *Water Hyacinth* Root	This paper	Cd(II)	77.2 mg g^{-1}
Biochar from *Water Hyacinth* Stem			87.20 mg g^{-1}

Fig. 5. Effect of electrolyte strength on adsorption performance in solution.

of these cations may affect the adsorption of Cd^{2+} by biochar [42], Na^+ ion was chosen as the representative to study the effect of ionic strength on the adsorption performance of biochar. The effect of electrolyte $NaNO_3$ concentration on the adsorption of Cd^{2+} by biochar RBC and SBC at 25ºC were shown in Fig. 5.

The dependence of biochar adsorption performance on ion concentration is usually divided into inner sphere (independent) and outer sphere (dependent) adsorption mechanisms [43]. When biochar is adsorbed by the inner sphere, the cation has no competition for the position inside the sphere; when adsorbed by the outer sphere, cations such as Na^+, Ca^{2+} and Al^{3+} can compete with the target ion to form the outer sphere surface complex, thus reducing the adsorption efficiency of target ions [44]. In this experiment, with the increase of electrolyte $NaNO_3$ concentration, the adsorption capacity of biochar RBC and SBC to Cd^{2+} decreased first, then increased, and finally tended to be stable. This may be due to that when the concentration of electrolyte in the solution is low, the biochar is mainly adsorbed by the outer sphere, which leads to the thickness of the electric double layer in the biochar is compressed, and the electrostatic interaction between Cd^{2+} and biochar is reduced, inhibiting the adsorption of Cd^{2+} by biochar. In addition, electrolyte ions compete with Cd^{2+}, and may even form complexes outside the adsorbent sphere, affecting the adsorption of Cd^{2+} by biochar [45]. When the electrolyte concentration increases further and reaches 0.05 mol·L^{-1}, the adsorption capacity of biochar to Cd^{2+} increases slightly, which may be due to the formation of surface complexes between Cd^{2+} and anions, or the change of surface charge of biochar after the ionic strength increases to a certain extent, resulting in the change of adsorption performance [46].

Previous studies have also found the same phenomenon and put forward the hypothesis that the ionic strength of the medium has an inflection point [47].

Equilibrium Adsorption Isotherms

Fig. 6 exhibits the equilibrium adsorption isotherms for RBC and SBC adsorption towards Cd carried out at different temperatures. SBC showed good adsorption effect at 25ºC, 35ºC and 45ºC, and the adsorption rate was above 99.60% for solutions with initial Cd^{2+} concentration lower than 30.00 mg L^{-1}. At 25ºC, the initial concentration of Cd^{2+} in the solution was increased, the adsorption capacity of biochar increased at the beginning. When the concentration reached to 10.00 mg L^{-1}, the adsorption capacity of RBC was 7.28 mg g^{-1}. As the concentration of Cd^{2+} in solution continues to increased, the adsorption capacity of RBC tends kept stable. At 35ºC and 45ºC, the equilibrium adsorption capacity of RBC to Cd^{2+} increases gradually with the increasing initial concentration. At 35ºC, the adsorption capacity of RBC to Cd^{2+} solution of 30.00 mg L^{-1} was 28.23 mg g^{-1}, and the adsorption rate was 94.11%. At 45ºC, the adsorption capacity of RBC to Cd^{2+} solution of 30.00 mg L^{-1} was 29.97 mg g^{-1}, and the adsorption rate can was 99.89%.

The isothermal curves of RBC and SBC were fitted nonlinearly. Fig. 6 revealed the relationship between Cd equilibrium concentration and saturated adsorption capacity for biochars from *Water Hyacinth*. The fitting parameters of RBC and SBC were showed in Table 3 and Table 4, respectively. From the parameter Tables 3 and 4, it can be seen that Langmiur model has a better fitting effect on RBC and SBC adsorption.
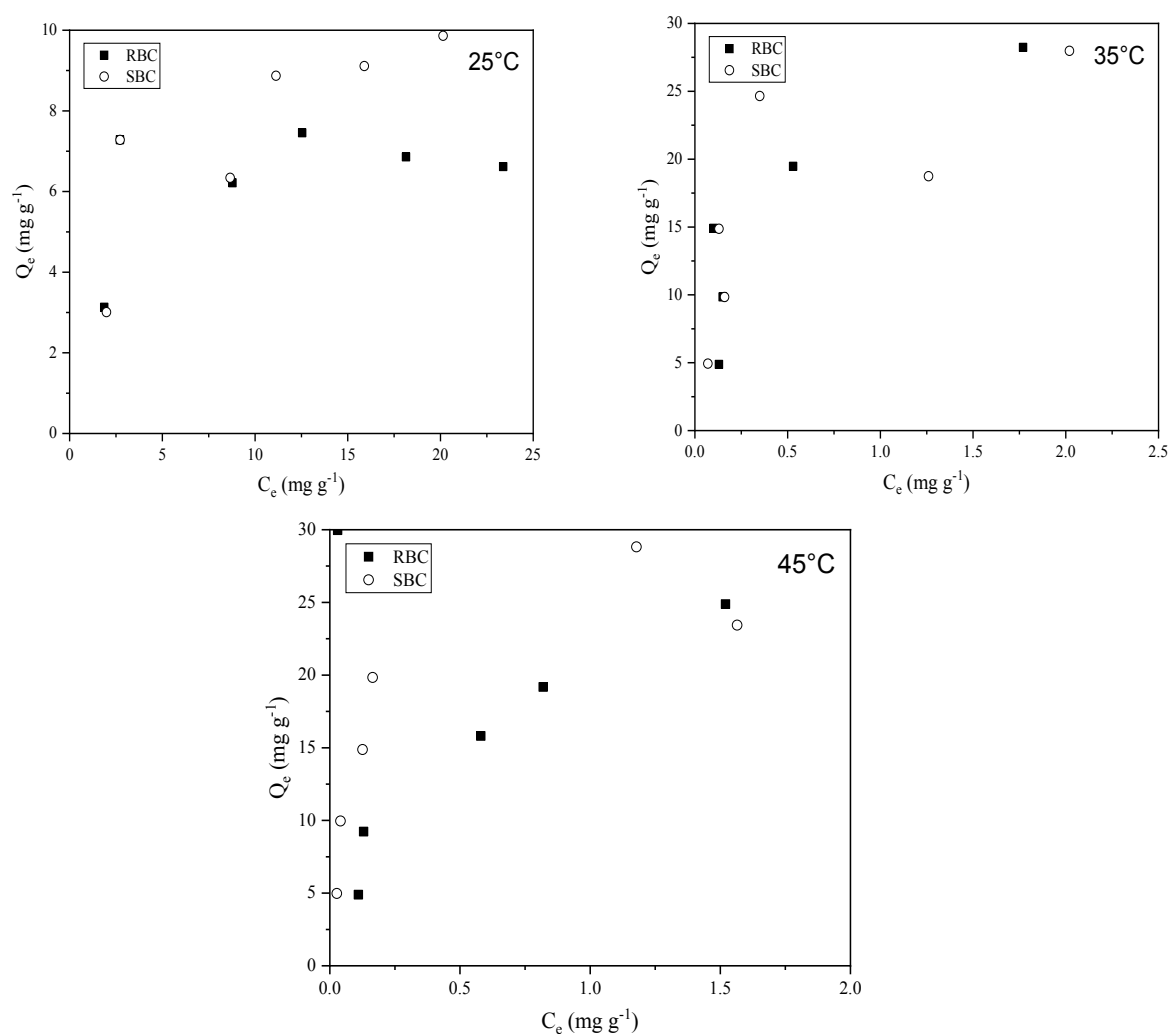
Fig. 6. The relationships between Cd equilibrium concentration and saturated adsorption capacity of RBC and SBC at different temperatures.

Table 3. Langmuir and Freundlich fitting parameters of RBC.

Temperature	Langmuir isotherm fitting			Freundlich isotherm fitting		
	R^2	b(L·g⁻¹)	Q_m (mg·g⁻¹)	R^2	K_F	n
25ºC	0.983	1.118	7.107	0.389	20.50	2.914
35ºC	0.838	4.702	25.316	0.568	895.78	2.999
45ºC	0.901	3.456	28.091	0.042	653.88	10.707

Table 4. Langmuir and Freundlich fitting parameters of SBC.

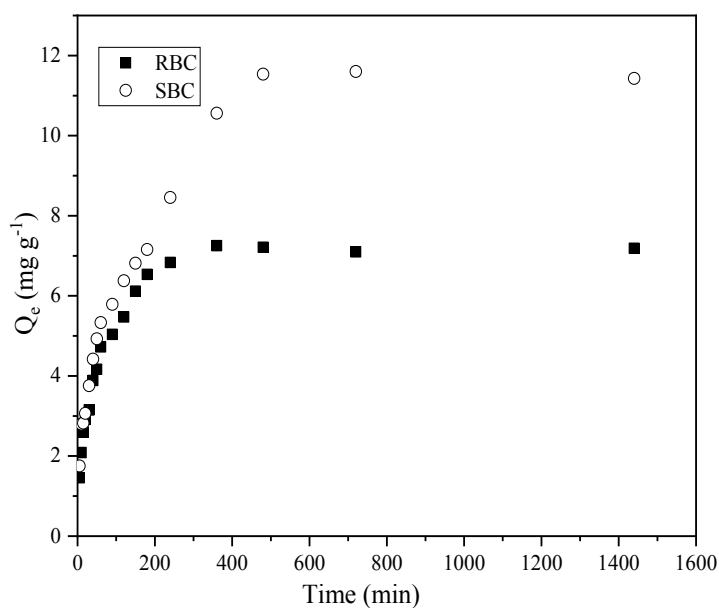| Temperature	Langmuir isotherm fitting			Freundlich isotherm fitting		
	R^2	b(L·g⁻¹)	Q_m (mg·g⁻¹)	R^2	K_F	n
25ºC	0.931	0.222	11.765	0.660	15.192	2.644
35ºC	0.921	4.046	28.409	0.832	1291.22	2.539
45ºC	0.979	13.5	26.455	0.807	1835.27	2.90

Fig. 7. Adsorption kinetics of Cd(II) ions onto SBC and RBC at 25ºC

The Langmuir isotherm assumes that the surface of the adsorbent is uniform and there is no interaction between adjacent sites in the adsorbate molecules. The Freundlich adsorption model is an empirical equation, assuming that metal ions are multi-layered on heterogeneous surfaces. Comparing the fitting parameters, it is found that the Langmiur adsorption model can better fit the adsorption process, and with the increase of adsorption temperature, the Q_m value of the adsorption model in Langmuir gradually increases except for SBC at 45ºC, which is basically consistent with the experimental results. It is indicated that the adsorption of heavy metals by *Water Hyacinth* biochar is a kind of chemisorption at the monolayer, while the Q_m value fitted by Langmuir model is close to the actual value.

Combined with the EDS results in Fig. 2, metal ions such as Ca^{2+}, Mg^{2+}, Al^{3+} are observed on the biochar. It can be concluded that these metal ions could be exchanged by Cd^{2+} in solution during sorption process due to direct electrostatic cation exchange, or metal exchange reactions with carboxyl and hydroxyl groups as well as co-precipitation [48]. Correspondingly, metal ion exchange has been suggested as a major mechanism for metal sorption by biochar.

Adsorption Kinetics

The plots of Q_e against t for different biochar materials at 25ºC are shown in Fig. 7. Fitting kinetics parameters of Cd(II) adsorption on SBC and RBC according to pseudo-first-order and pseudo-two-order models are tabulated in Table 5.

The results show that two models fit the experimental data quite well due to the R^2 values exceed 0.950. However, notable variances between the experimental and theoretical uptakes reveal the adsorption behavior is not a first-order reaction [49]. By comparison, the higher correlation coefficients ($R^2 > 0.990$) indicated that uptakes of Cd(II) onto SBC and RBC can be well represented by the pseudo-second-order model. The calculated Q_e values (12.136 mg g^{-1} of SBC for Cd(II), and 7.386 mg g^{-1} of SBC for Cd(II)) were very close to the experimental data (12.186 mg g^{-1} of SBC for Cd(II), and 7.397 mg g^{-1} of SBC for Cd(II)). Moreover, the initial adsorption rate (v_0) of RBC (0.252 mg g^{-1} min^{-1}) is larger than SBC (0.170 mg g^{-1} min^{-1}) according to the linear fitting. The results indicate the applicability of pseudo-second-order model to describe the adsorption behavior, and the two biochars show significant differences in the initial adsorption rates and heavy metal uptakes.

Table 5. The Kinetic fitting parameters of Cd(II) ions Uptake onto SBC and RBC.

Biochars	The pseudo-first-order model fitting			The pseudo-second-order model fitting		
	R^2	k_1 (min^{-1})	Q_e(mg g^{-1})	R^2	k_2 (g mg^{-1} min^{-1})	Q_e(mg g^{-1})
SBC	0.970	0.00461	9.931	0.993	0.00116	12.140
RBC	0.953	0.00967	5.560	0.999	0.00461	7.386

Leaching Characteristics of Alkali (earth) Metal in Biochar

The alkali (earth) metals in biochar mainly come from the nutrients absorbed during the growth of biomass, and mainly exist in biochar in the form of ionic salts, among which K, Mg and Ca have certain effects on the adsorption performance of biochar. Studies have shown that it can form coprecipitation with heavy metals in solution to remove heavy metals, and can also serve as an adsorption site to enhance the adsorption effect of biochar on heavy metals [50].

Leaching Rule of Alkali (earth) Metal in Biochar at Different Initial Concentrations

The change of leaching amount of alkali (earth) metal with the increase of initial concentration of Cd^{2+} in solution were shown in Fig. 7.

The leaching amount of K^+, Ca^{2+} and Mg^{2+} in SBC was basically consistent with the increase of the initial concentration of Cd^{2+} in the solution, and increased with the increase of the initial concentration of Cd^{2+}, indicating that the presence of alkali (earth) metals in biochar was correlated with its adsorption capacity.
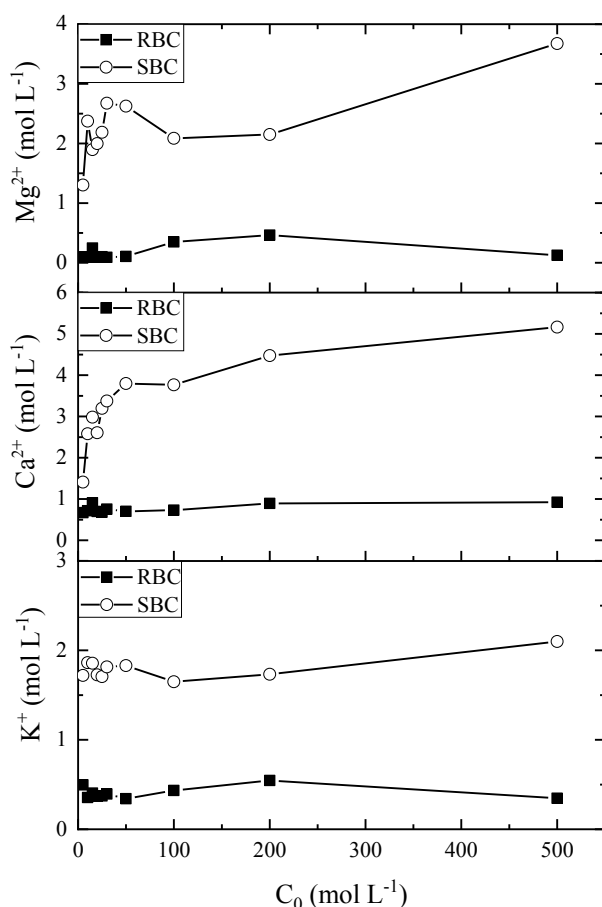

Fig. 8. Leaching of alkali (earth) metals in RBC and SBC at different initial concentrations.

The leaching amount of Mg^{2+} in RBC increases with the increase of the initial concentration of Cd^{2+} in solution, and the leaching amount of K^+ and Ca^{2+} shows similar trends, when the initial concentration of Cd^{2+} reaches to 200.00 mg L^{-1}, reaching the maximum value 0.59 mg·g^{-1} and 0.49mg·g^{-1}, respectively. The initial concentration of Cd^{2+} continues to increase, while the leaching amount of K^+ and Ca^{2+} decreases slightly. In addition, when the initial concentration of Cd^{2+} in solution is the same, the leaching amount of three ions in SBC was obviously larger than that in RBC, which was consistent with the conclusion that the content of Mg and Ca in SBC is higher than that in RBC in EDS elemental analysis, and may be related to the larger specific surface area of SBC.

Effect of Ionic Strength on Leaching of Alkali (earth) Metal in Biochar

The effect of electrolyte strength on alkali (earth) metal leaching in RBC and SBC were shown in Fig. 9. It can be seen that with the increase of electrolyte concentration in the solution, the equilibrium concentrations of alkaline earth metal ions K^+, Mg^{2+} and Ca^{2+} in RBC show a trend of decreasing at first and then increasing. Combined with the foregoing, it can be seen that the increase of ionic strength in the solution not only affects the adsorption of heavy metals by biochar, but also affects the release of alkaline earth metals in biochar. When the concentration of electrolyte in solution was 0.10 mol L^{-1}, the leaching amount of three alkaline earth metals in RBC was the lowest, and the leaching trend of Mg^{2+} and Ca^{2+} was similar to that of RBC for adsorbing Cd^{2+}. In contrast, the leaching amount of alkali metal K^+ in SBC was much higher than that of alkaline earth metal Mg^{2+} and Ca^{2+}, which may be due to the high content of K in raw materials. The maximum amount of K^+ leaching can reach 147.35 mg g^{-1}, and the leaching amount shows a trend of increasing first, then decreasing and gradually stabilizing. The leaching amount of Mg^{2+} and Ca^{2+} has a similar trend, which is gradually increasing and tends to be stable. The maximum leaching amount of Mg^{2+} is 7.67 mg g^{-1}, and the maximum leaching amount of Ca^{2+} is 7.17 mg g^{-1}.

Correlation Analysis between Alkali (earth) Metal Leaching and Biochar Adsorption

Correlation between Initial Concentration and Alkali (earth) Metal Leaching from Biochar

The correlation between the leaching of alkali (earth) metal and the biochar adsorption performance of RBC and SBC in different Cd^{2+} initial concentration solutions are shown in Tables 6 and 7. The correlation analysis showed that the adsorbability of RBC and SBC to Cd^{2+} was positively correlated with the leaching amount of Mg^{2+} and the correlation degree was SBC>RBC
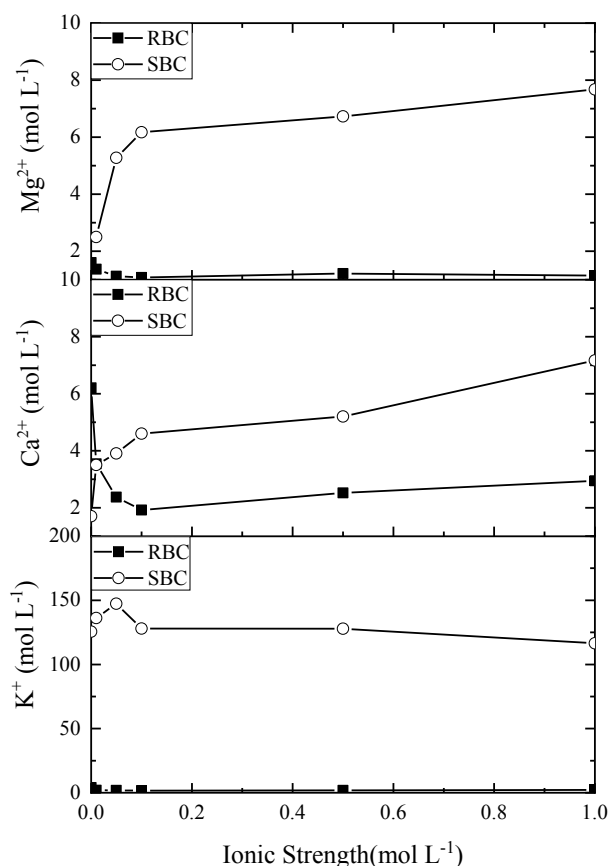
Fig. 9. Effect of electrolyte strength on alkali (earth) metal leaching in solution.

with correlation coefficients of 0.849** and 0.724*, respectively. The results are completely consistent with the adsorption effect of the two kinds of biochar, indicated that when the alkaline earth metal Mg^{2+} in the biochar is released into the solution, the vacancy points on the surface of the biochar are exposed, which can replace the heavy metals in the solution.

As shown in Tables 6 and 7, the release of alkaline earth metal Mg^{2+} is not only positively correlated with the concentration of heavy metals in the solution, but also positively correlated with other alkali metals and alkaline earth metals. The leaching of Mg^{2+} in RBC is significantly positively correlated with leaching of K^+ and Ca^{2+}, with correlation coefficients of 0.891** and 0.947**, respectively. The leaching of Mg^{2+} in SBC is mainly positively correlated with the leaching of Ca^{2+}, with a correlation coefficient of 0.803**; It can be concluded that the leaching of Mg^{2+} is synchronous with the leaching of K^+ and Ca^{2+}.

Cluster Analysis

Cluster Analysis (HCA) is a method of data verification that divides all paradigms into smaller clusters or based on how similar they are to other groups. The smaller the distance between the samples, the more similar they are. Cluster analysis diagrams of RBC and SBC are based on the data of Mg^{2+} leaching, which were shown in Fig. 10., respectively. The evolutionary tree represents the similarities and differences between various factors in Mg^{2+} leaching

Table 6. Correlation between initial concentration of Cd^{2+} in solution and alkali (earth) metal leaching in RBC.

Correlation					
	RBC	Cd^{2+}	K^+	Mg^{2+}	Ca^{2+}
RBC	1	0.901**	0.006	0.669*	0.218
Cd^{2+}		1	0.351	0.724*	0.557
K^+			1	0.891**	0.823**
Mg^{2+}				1	0.947**
Ca^{2+}					1

** . Significant correlation was found at 0.01 level (bilateral).   * . Significant correlation was found at 0.05 level (bilateral).

Table 7. Correlation between initial concentration of Cd^{2+} in solution and alkali (earth) metal leaching in SBC.

Correlation					
	SBC	Cd^{2+}	K^+	Mg^{2+}	Ca^{2+}
SBC	1	0.895**	0.684*	0.800**	0.751*
Cd^{2+}		1	0.424	0.849**	0.575
K^+			1	0.822**	0.793*
Mg^{2+}				1	0.803**
Ca^{2+}					1

** . Significant correlation was found at 0.01 level (bilateral).   * . Significant correlation was found at 0.05 level (bilateral).
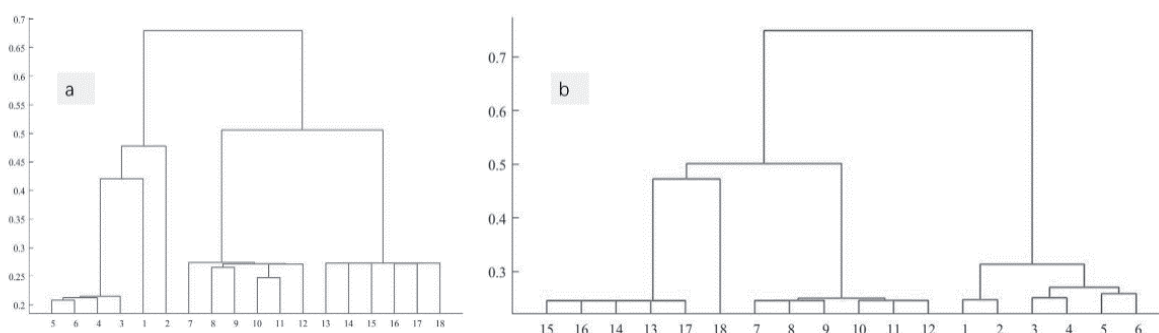
Fig. 10. Cluster analysis of a) RBC and b) SBC.

ability. Among them, 1, 2, 3, 4, 5, and 6 in Fig. 10 indicated that the initial concentration of Cd^{2+} in the solution were 5.00, 10.00, 15.00, 20.00, 25.00, and 30.00 mg L^{-1} at a temperature of 25ºC, respectively, and cluster analysis of leaching of Mg^{2+} and adsorption of Cd^{2+} in RBC and SBC. Seen from Fig. 10, 7, 8, 9, 10, 11, and 12 indicated that the initial concentration of Cd^{2+} in the solution were 5.00, 10.00, 15.00, 20.00, 25.00, and 30.00 mg L^{-1} at a temperature of 35ºC, respectively, and cluster analysis of leaching of Mg^{2+} and adsorption of Cd^{2+} in RBC and SBC. 13, 14, 15, 16, 17, and 18 in Fig. 10 indicated that the initial concentration of Cd^{2+} in the solution were 5.00, 10.00, 15.00, 20.00, 25.00, and 30.00 mg L^{-1} at a temperature of 45 ˚C, respectively, and cluster analysis of leaching of Mg^{2+} and adsorption of Cd^{2+} in RBC and SBC.

At 25ºC, 35ºC and 45ºC, the leaching amounts of alkaline earth metals Mg^{2+} of RBC and SBC in solutions with different initial concentrations of Cd^{2+} form three clusters, and the clusters formed at 35ºC and 45 ˚C were the same category, indicating that there was little difference in the leaching capacity of alkaline earth metal Mg^{2+} at these two temperatures, while the largest difference was the clusters formed at 25ºC.

Regeneration of Biochar Adsorbents and Economic Assessment

Regeneration experiments were carried out using a commonly utilized alkaline washing method used for obtaining biochar-based carbonaceous adsorbents. It is researched that desorption rate (%) of Cd(II) by disruption the coordination of metal ions and subsequent release from the material surface into the basic solution. The results relating to the regeneration of Cd(II) by desorption cycle are shown in Figure 11. In the chemical regeneration trials, the desorption rate increased in the first test and then decreased gradually with each subsequent regeneration cycle. The decreasing trends were largely due to the structural deterioration of the adsorbents during the continuous regeneration process [51, 52]. However, both weight loss and desorption rate reduction were not remarkable. The rate of the biochar regeneration was over 80% for five cycles. After five

usages, the regeneration efficiency of RBC slightly decreased to 86.33% compared to the peak value, which is higher than the maximum of SBC (85.64%) after the third cycle. The better desorption rate of RBC should be ascribed to the rich root structure. On the whole, the findings show the promising possibility of the NaOH regeneration of the SBC and RBC adsorption for Cd(II).

The use of *Water Hyacinth* biochar in heavy metal treatment could provide a chance for turning into a valuable resource, as well as benefiting the socio-economic value of the whole ecology. In addition, the wide source for SBC and RBC combined with no need for activation process further enable the engineering implication possible. Globally, the mean price for biochars was $2.65 kg^{-1}, which ranged from as low as $0.09 kg^{-1} to as high as $8.85 kg^{-1} [53]. Investigations reveal commercial grade carbon absorbent costs almost $0.54 kg^{-1} in Chinese market. After considering the cost of cultivation, pretreatment, carbonization, and adsorption, the cost of SBC and RBC prepared from *Water Hyacinth* and adsorbing Cd(II) in this research is approximately $0.25 kg^{-1}. Hence, this carbonaceous
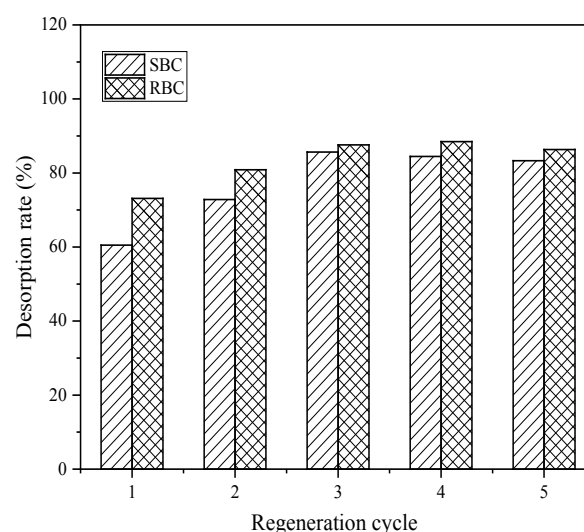

Fig. 11. Effect of HCl concentration on desorption of Pb(II) and Zn(II).

material would be a commercial alternative with a certain economic value in removing heavy metal from aqueous solutions.

Conclusion

In this paper, biochar was prepared by pyrolysis of *Water Hyacinth* biomass to study the characteristics of biochar and its adsorption mechanism on Cd^{2+}. It is indicated that it is feasible to remove the heavy metal Cd^{2+} in wastewater by *Water Hyacinth* biochar, and the following conclusions were drawn.

Firstly, the physical and chemical properties of biochar prepared from different parts of *Water Hyacinth* are different. The yield of biochar prepared from stem is lower than that from root. The pore structure of SBC is rich and the crystal structure is different, and the adsorption performance of SBC is better than that of RBC.

Secondly, the adsorption capacity of *Water Hyacinth* biochar increased with the increase of initial concentration of Cd^{2+} in the solution. When the initial concentration reached 200.00 $mg \cdot L^{-1}$, the adsorption capacity gradually stabilized; and the increase of temperature was also beneficial to the adsorption of Cd^{2+} by *Water Hyacinth* biochar. The adsorption isotherm curves of RBC and SBC adsorbing Cd(II) can be well fitted by Langmiur adsorption model. The kinetics simulated by the relation between the adsorption capacity and equilibrium Cd(II) concentration is admirably explained by the pseudo-second-order model. The results show that there are adsorption sites on the inner and outer surfaces of *Water Hyacinth* biochar, and the adsorption process is multi-molecular layer adsorption

Finally, the adsorption effect of RBC and SBC on Cd^{2+} in solution is positively correlated with the amount of leaching of alkaline earth metal Mg^{2+}, indicating that the leaching amount of alkaline earth metal Mg^{2+} in biochar is affected by Cd^{2+} concentration. The leaching amount of Mg^{2+} in SBC is larger than RBC, and the adsorption effect is stronger than RBC, which proves that the release of alkaline earth metal Mg^{2+} in biochar is beneficial to the adsorption of Cd^{2+} by biochar.

Due to high recovery and advantageous economic cost, *Water Hyacinth* can be used to treat wastewater stream containing large amounts of Cd(II).

Conflict of Interest

The authors declare no conflict of interest.

References

1. MA X.L., ZOU H., TIAN M.J., ZHANG L.Y., MENG L., ZHOU X.N., MIN N., CHANG X.Y., LIU Y. Assessment of heavy metals contamination in sediments from three adjacent regions of the Yellow River using metal chemical fractions and multivariate analysis techniques. Chemosphere, **144**, 264, **2016**.
2. YANG X., WAN Y., ZHENG Y., HE F., YU Z., HUANG J., WANG H., OK Y.S., JIANG Y., GAO B. Surface functional groups of carbon-based adsorbents and their roles in the removal of heavy metals from aqueous solutions: A critical review. Chemical Engineering Journal, **366**, 608, **2019**.
3. STRONG R.J. HALSALL C.J., FERENCIK M., JONES K.C., SHORE R.F., MARTIN F.L. Biospectroscopy reveals the effect of varying water quality on tadpole tissues of the common frog (Rana temporaria). Environmental Pollution. **213**, 322-337, **2016**.
4. KIM S.U., OWENS V.N., KIM S.Y., HONG C.O. Effect of different way of bottom ash and compost application on phytoextractability of cadmium in contaminated arable soil. Applied Biological Chemistry, **60**, 353, **2017**.
5. ZOU Y., WANG X., KHAN A., WANG P., LIU Y., ALSAEDI A., HAYAT T., WANG X. Environmental Remediation and Application of Nanoscale Zero,Valent Iron and Its Composites for the Removal of Heavy Metal Ions: A Review. Environmental Science & Technology, **50** (14), 7290, **2016**.
6. MORCILLO P., ESTEBAN M., CUESTA A. Heavy metals produce toxicity, oxidative stress and apoptosis in the marine teleost fish SAF-1 cell line. Chemosphere, **144**, 225-233, **2016**.
7. KIM D.J., SHIN H.J., AHN B.K., LEE J.H. Competitive adsorption of thallium in different soils as influenced by selected counter heavy metals. Applied Biological Chemistry, **59(5)**, 695, **2016**.
8. GUO X., HUANG D., LIU Y., PENG Z., ZENG G., XU P., CHENG M., WANG R., WAN J. Remediation of contaminated soils by biotechnology with nanomaterials: bio-behavior, applications, and perspectives. Critical Reviews in Biotechnology, **38** (3), 455, **2018**.
9. MOHAN D., JR C.U.P., BRICKA M., SMITH F., YANCEY B., MOHAMMAD J., STEELE P.H., ALEXANDRE-FRANCO M.F., GOMEZ-SERRANO V., GONG H. Sorption of arsenic, cadmium, and lead by chars produced from fast pyrolysis of wood and bark during bio-oil production. Journal of Colloid & Interface Science, **310** (1), 57, **2007**.
10. OLIVARES H.G., LAGOS N.M., GUTIERREZ C.J., KITTELSEN R.C., VALENZUELA G.L., LILLO M.E.H.

Assessment oxidative stress biomarkers and metal bioaccumulation in macroalgae from coastal areas with mining activities in Chile [J]. Environmental Monitoring and Assessment, **188**, 25, **2016**.

11. POREBA R., GAC P., POREBA M., DERKACZ A., PILECKI W., ANTONOWICZ-JUCHNIEWICZ J., ANDRZEJAK R. Relationship between chronic exposure to lead, cadmium and manganese, blood pressure values and incidence of arterial hypertension [J]. Medycyna Pracy, **61** (1), 5-14, **2010**.

12. WANG L., WANG Y., MA F., TANKPA V., BAI S., GUO X., WANG X. Mechanisms and reutilization of modified biochar used for removal of heavy metals from wastewater: A review. Science of The Total Environment, **668**, 1298, **2019**.

13. FU F., WANG Q. Removal of heavy metal ions from wastewaters: A review. Journal of Environmental Management, **92** (3), 407, **2011**.

14. WAN S., WU J., ZHOU S., WANG R., GAO B., HE F. Enhanced lead and cadmium removal using biochar, supported hydrated manganese oxide (HMO) nanoparticles: Behavior and mechanism. Science of The Total Environment, **616-617**, 1298, **2018**.

15. CUI X., FANG S., YAO Y., LI T., NI Q., YANG X., HE Z. Potential mechanisms of cadmium removal from aqueous solution by *Canna indica* derived biochar. Science of The Total Environment, **562,** 517, **2016**.

16. WANG S., GAO B., ZIMMERMAN A.R., LI Y., MA L., HARRIS W.G., MIGLIACCIO K.W. Removal of arsenic by magnetic biochar prepared from pinewood and natural hematite. Bioresource Technology, **175**, 391, **2015**.

17. INYANG M.I., GAO B., YAO Y., XUE Y., ZIMMERMAN A., MOSA A., PULLAMMANAPPALLIL P., OK Y.S., CAO X. A Review of Biochar as a Low-Cost Adsorbent for Aqueous Heavy Metal Removal. Critical Reviews in Environmental Science & Technology, **46** (4), 406, **2016**.

18. GUPTA V.K., MORADI O., TYAGI I., AGARWAL S., SADEGH H., SHAHRYARI-GHOSHEKANDI R., MAKHLOUF A.S.H., GOODARZI M., GARSHASBI A. Study on the removal of heavy metal ions from industry waste by carbon nanotubes: Effect of the surface modification: A review. Critical Reviews in Environmental Science & Technology, **46** (2), 93, **2016**.

19. WANG L., WANG Y., MA F., TANKPA V., BAI S., GUO X., WANG X. Mechanisms and reutilization of modified biochar used for removal of heavy metals from wastewater: A review. Science of the Total Environment, **668**, 1298, **2019**.

20. HUR J.R., JHO E.H. Effect of hemoglobin on the growth and Cd accumulation of pea plants (Pisum sativum L.). Applied Biological Chemistry, **60**, 673, **2017**.

21. LI H., DONG X., SILVA E.B.D., OLIVEIRA L.M.D., CHEN Y., MA L.Q. Mechanisms of metal sorption by biochars: Biochar characteristics and modifications. Chemosphere, **178**, 466, **2017**.

22. LIU S., ZENG G., NIU Q., LIU Y., ZHOU L., JIANG L., TAN X., XU P., ZHANG C., CHENG M. Bioremediation mechanisms of combined pollution of PAHs and heavy metals by bacteria and fungi: A mini review. Bioresource Technology, **224**, 25, **2017**.

23. KOLODYNSKA D., KRUKOWSKA J., THOMAS P. Comparison of Sorption and Desorption Studies of Heavy Metal Ions From Biochar and Commercial Active Carbon. Chemical Engineering Journal, **307**, 353, **2017**.

24. MASTO R.E., KUMAR S., ROUT T.K., SARKAR P., GEORGE J., RAM L.C. Biochar from *Water Hyacinth* (Eichornia crassipes) and its impact on soil biological activity. Catena, **111**, 64, **2013**.

25. MURAMOTO S., OKI Y. Removal of some heavy metals from polluted water by *Water Hyacinth* (Eichhornia crassipes). Bulletin of Environmental Contamination & Toxicology, **30**, 170, **1983**.

26. XIE Y., YU D. The significance of lateral roots in phosphorus (P) acquisition of *Water Hyacinth* (*Eichhornia crassipes*). Aquatic Botany, **75** (4), 311, **2003**.

27. BOGUSZ A., OLESZCZUK P., DOBROWOLSKI R. Application of laboratory prepared and commercially available biochars to adsorption of cadmium, copper and zinc ions from water. Bioresource Technology, **196**, 540, **2015**.

28. WANG H., GAO B., WANG S., FANG J., XUE Y., YANG K. Removal of Pb(II), Cu(II), and Cd(II) from aqueous solutions by biochar derived from KMnO$_4$ treated hickory wood. Bioresource Technology, **197**, 356, **2015**.

29. CUI X., FANG S., YAO Y., LI T., NI Q., YANG X., HE Z. Potential mechanisms of cadmium removal from aqueous solution by Canna indica derived biochar. Science of the Total Environment, **562**, 517, **2016**.

30. PENG Z.D., LIN X.M., ZHANG Y.L., HU Z., YANG X.J., CHEN C.Y., CHEN H.Y., LI Y.T., WANG J.J. Removal of cadmium from wastewater by magnetic zeolite synthesized from natural, low-grade molybdenum. Science of The Total Environment, **772**, 145355, **2021**.

31. BORDOLOI S., GRAG A., SREEDEEP S., LIN P., MEI G. Investigation of cracking and water availability of soil-biochar composite synthesized from invasive weed *Water Hyacinth*. Bioresource Technology, **263**, 665, **2018**.

32. LIU W., LI W., JIANG H., YU H. Fates of Chemical Elements in Biomass during Its Pyrolysis. Chemical Reviews, **117** (9), 6367, **2017**.

33. UCHIMIYA M. Influence of pH, ionic strength, and multidentate ligand on the interaction of Cd^{II} with biochars. Acs Sustainable Chemistry & Engineering, **2** (8), 2019, **2014**.

34. TULYAGANOV D.U., RIBEIRO M.J., LABRINCHA J.A. Development of glass-ceramics by sintering and crystallization of fine powders of calcium- magnesium-aluminosilicate glass. Ceramics International, **28** (5), 515, **2002**.

35. HOU J., SUO Q., LIU M., ZHAO L., LIU X., XING H., CHEN Y. Effects of carbonization temperature on the pH and of K, Ca and Mg concentrations in biochar. Science & Technology Review, **33** (5), 88, **2015**.

36. BULGARIU D., BULGARIU L., FILIPOV F., ASTEFANEI D., STOLERU V. Selective Separation and Determination of Heavy Metals (Cd, Pb, Cr) Speciation Forms from Hortic Antrosols. Journal of Gastroenterology, **42** (1), 39, **2009**.

37. SABELA M.I., KUNENE K., KANCHI S., XHAKAZA N.M., BATHINAPATLA A., MDLULI P., SHARMA D., BISETTY K. Removal of copper (II) from wastewater using green vegetable waste derived activated carbon: An approach to equilibrium and kinetic study. Arabian Journal of Chemistry, **12**, 4331, **2016**.

38. JOSEPH I.V., TOSHEVA L., DOYLE A.M. Simultaneous removal of Cd(II), Co(II), Cu(II), Pb(II), and Zn(II) ions from aqueous solutions via adsorption on FAU-type zeolites prepared from coal fly ash. Journal of Environmental Chemical Engineering, **8** (4), 103895, **2020**.

39. GUPTA S., BABU B.V. Removal of toxic metal Cr(VI) from aqueous solutions using sawdust as adsorbent:

Equilibrium, kinetics and regeneration studies. Chemical Engineering Journal, **150** (2-3), 352, **2009**.

40. ASANDEI D., BULGARIU L, BOBU E. Lead (II) removal from aqueous solutions by adsorption onto chitosan. Cellulose Chemistry & Technology, **43** (4-6), 211, **2009**.

41. XU X., CAO X., ZHAO L., WANG H., YU H., GAO B. Removal of Cu, Zn, and Cd from aqueous solutions by the dairy manure-derived biochar. Environmental Science and Pollution Research, 20, 358, **2013**.

42. DONG L., ZHU Z., QIU Y., ZHAO J. Removal of lead from aqueous solution by hydroxyapatite/magnetite composite adsorbent. Chemical Engineering Journal, **165** (3), 827, **2010**.

43. PARK J.H., OK Y.S., KIM S.H., CHO J.S., HEO J.S., DELAUNE R.D., DEO D.C. Competitive adsorption of heavy metals onto sesame straw biochar in aqueous solutions. Chemosphere, **142**, 77, **2016**.

44. GUO X., ZHANG S., SHAN X. Adsorption of metal ions on lignin. Journal of Hazardous Materials, **151** (1)**,** 134, **2008**.

45. LI Z., KATSUMI T., IMAIZUMI S., TANG X., INUI T. Cd(II) adsorption on various adsorbents obtained from charred biomaterials. Journal of Hazardous Materials, **183** (1-3), 410, **2010**.

46. SUN J., LIAN F., LIU Z., ZHU L., SONG Z. Biochars derived from various crop straws: Characterization and Cd(II) removal potential. Ecotoxicology and Environmental Safety, **106**, 226, **2014**.

47. LIU H., ZHANG W., YANG Y., HUANG X., WANG S., QIU R. Relative distribution of Pb^{2+} sorption mechanisms by sludge,derived biochar. Water Research, **46** (3), 854, **2012**.

48. CUI X., FANG S., YAO Y., LI T., NI Q., YANG X., HE Z. Potential mechanisms of cadmium removal from aqueous solution by Canna indica derived biochar. Science of the Total Environment, **562**, 517, **2016**.

49. YOUSEF R.I., El-ESWED B., AL-MUHTASEB A.A.H. Adsorption characteristics of natural zeolites as solid adsorbents for phenol removal from aqueous solutions: Kinetics, mechanism, and thermodynamics studies. Chemical Engineering Journal, **171** (3), 1143, **2011**.

50. MACKAY A.A., VASUDEVAN D. Polyfunctional Ionogenic Compound Sorption: Challenges and New Approaches To Advance Predictive Models. Environmental Science & Technology, **46** (17), 9209, **2012**.

51. VIJAYARAGHAVAN K., JEGANB J., PALANIVELU K., VELAN M. 2005. Biosorption of copper, cobalt and nickel by marine green alga Ulva reticulata in a packed column. Chemosphere, **60**, 419, **2005**.

52. LEE C.G., JEON J.W., HWANG M. J., AHN K.H., PARK C., CHOI J.W., LEE S.H. Lead and copper removal from aqueous solutions using carbon foam derived from phenol resin. Chemosphere, **130**, 59, **2015**.

53. AHEMD M.B., ZHOU J.L., NGO H.H., GUO W. Insight into biochar properties and its cost analysis. Biomass Bioenergy, **84**, 76-86, **2016**.